THE AMERICAN SOCIETY OF MECHANICAL ENGINEERS
345 E. 47th St., New York, N.Y. 10017

95-GT-378

INTERSTAGE DISK-CAVITY/BRUSH SEAL NUMERICAL FLOW VISUALIZATION STUDY

V.V. Kudriavtsev, M.J. Braun

Department of Mechanical Engineering
The University of Akron, Akron, Ohio, 44325

ABSTRACT

This paper presents work-in-progress results and model developments that are directed towards the computational fluid dynamics simulation of the secondary flow system in a gas turbine engine. Numerical flow visualization results of the 2-D axisymmetric rotational fluid flow ($Re=10^5$) in a generic cross section of an interstage turbine cavity are displayed. The core flow is driven by an imposed pressure drop along the vane row of the main flow path. Three interconnected disk cavities separated by a brush seal are located along the secondary flow path. A new computational algorithm was developed in order to predict the flow patterns and leakages for different seal and cavity configurations. The code is based on the numerical solution of the transient laminar Navier-Stokes equations, written in primitive variables and approximated on a nonuniform rectangular collocated grid. The program uses a mass and momentum conservative formulation as well as a set of boundary conditions for pressure and conservation of mass. The pressure solution uses the Poisson equation under a direct implementation procedure. A time dependent Alternating Direction Implicit(ADI) method is also used for the solution of all primitive variables. This integrated computational approach allows the simulation of the rotating disk cavity vortex flow periodic features, as well as their impact on leakage flow and sealing effectiveness. In the present study this approach is used to numerically investigate the flow through the brush. The main purpose of this study is to present an integrated brush seal/disk cavity flow model, to demonstrate the effectiveness of this approach, and to emphasize the necessity for further work in this direction.

NOMENCLATURE

d- brush seal bristle diameter
h - physical height of the cavity
l - physical length of the cavity
L_o - length scale, L_o=1 mm
U_o - velocity scale, velocity of the main flow stream(U_{in})
w_{max}- maximum rotational speed at the tip of the rotating disk
u- nondimensional axial speed $u=U/U_o$
v- nondimensional radial speed $v=V/U_o$
w-nondimensional rotational speed $w=W/U_o$
t - nondimensional time, $t=T/T_o$, $T_o = L_o/U_o$
p- nondimensional pressure, $p=P/\rho U_o^2$
Re - Reynolds number, $Re=(U_o L_o)/\nu$.
Re_m- main flow Reynolds number, $Re_m=(U_o l)/\nu$,
$Re_w=(W l)/\nu$
k-permeability coefficient
k-nondimensional permeability coefficient(Darcy number), $k=Da=k/L_o^2$
k_u-brush seal Darcy number
k_x- vane flow Darcy number
ϵ- porosity, $\epsilon=0$ in the area occupied by the fluid, $\epsilon=0.216$ in the brush seal area

1. INTRODUCTION

Recently, there has been a significant increase in the studies concerning the detailed physics of rotational flows in disk cavities, Przekwas et al., (1994), Virr et al., (1993), Athavale et al., (1993). One of the main motivations for studying this problem is its direct application to gas turbine

Presented at the International Gas Turbine and Aeroengine Congress and Exposition
Houston, Texas - June 5-8, 1995

secondary flow systems management, in particular the rim and interstage cavities. Improved efficiency of the gas turbine performance has been directly traced to improvements in the secondary flow path system, which can be simulated both through improved experimental, and novel computational methodologies.

A problem closely related to the current study is the flow in a cavity with rotating walls. This case has been extensively studied by Chew(1985), Farthing et al., (1992) and Ong and Owen(1991). Chew(1985) treated some fundamental aspects of the heat transfer in centrifugally driven, steady-state free convection flow in a cylindrical cavity with a non-uniform disk-temperature distribution. In numerical and experimental studies performed by Owen and his associates, a rotating cavity with axial cooling air throughflow was used for the determination of heat transfer(Ong and Owen, 1991), and flow structures(Farthing et al., 1992). Owen and Onur(1983) observed that at certain rotational velocities a non-axisymmetric vortex breakdown could occur and circulation inside the cavity becomes weaker as the Rossby number is reduced. The effect of the mainstream flow on the cavity flow has been studied numerically by Vaughan and Turner(1987). They showed that for certain conditions, a laminar 3-D solution gives a sinusoidally varying ingress-egress cycle in the rim seal area. Ko et al., (1993) studied the axisymmetric sub-problem of a generic rotor-stator cavity. This work illuminated the presence of the main flow induced recirculation zone in the cavity gap area. Athavale et al., (1993) performed numerical calculations to predict the rotational cavity flows with long clearance sections. The appearance of Taylor vortices was observed for supercritical rotational Reynolds numbers.

In the secondary flow systems, cavities are usually separated from the main stream, and each other by different types of seals, mostly labyrinths and honeycombs. There has been a number of previous studies that showed a marked improvement in sealing efficiency when the labyrinth seal was replaced by a brush seal, Carlile et al., (1993) and Chupp and Dowler (1993). Unfortunately, to date, brush seal theory has not been developed extensively, and a reliable numerical model that would allow widespread parametric design is still missing. Very few of the previous studies of this type of seal have involved theoretical, and numerical work. Most of the existing studies are experimental in nature. Chupp, et. al., (1991,1994) and Hendricks et. al., (1991) pioneered a simple theoretical leakage flow model through the brush seal. However, simple models can not fully account for the effects of changes in the details of the brush geometries. The only availahle numerical simulations that analyze brush seal flows based on the composition of the brush are those of Braun and Kudriavtsev(1992, 1993a,b), and Kudriavtsev (1993). In these works the brush seal was simulated as a segment of densely packed cylinders, and the Navier-Stokes equations were directly applied to the flow upstream, in-between, and downstream of these cylinders, Fig. 2. These studies demonstrated that although fluid flow through the brush can be successfully 'micro-modeled', such direct brush modeling can be prohibitively expensive computationally, Kudriavtsev and Braun (1994). These authors searched for improved computational methodologies which eventually allowed the development of several simplified numerical models, such as brush partitioning(Kudriavtsev and Braun, 1994), and brush representation by a variable porosity porous body.

All studies reviewed here were concerned with the cases when either the disk cavity, or the seal were analyzed separately. Hendricks (Przekwas et al., (1994)) proposed that these two components be integrated in one computational algorithm, thus increasing the physical accuracy of the simulation.

The brush body can be modeled approximately as a saturated porous medium using Darcy's formula

$$-\frac{\partial P}{\partial x} = \frac{\mu}{k} U \tag{1a}$$

and/or the Brinkman assumptions (Burmeister, 1993)

$$-\frac{\partial P}{\partial x} = \frac{\mu}{k} U - \frac{\mu}{\epsilon} \nabla^2 U \tag{1b}$$

where ϵ is the porosity of the porous media, k is the permeability, U is the speed, and P is the pressure .

In the present study this approach is used to investigate numerically the flow through the brush. The main purpose of this study is to present an integrated brush seal/disk cavity flow model, to demonstrate the effectiveness of this approach, and to emphasize the necessity for further work in this direction.

2. PROBLEM FORMULATION AND DETAILS OF THE SOLUTION PROCEDURE

The present study considers the fluid flow in a rotational interstage cavity(IC). Such cavity consists of a combination of the main flow path, front cavity with the rotating wall, stationary vane, and back cavity with a rotating wall. The cavities are separated by a brush seal affixed to the lower axial wall of the vane, Fig. 1a. The main flow is driven by a pressure drop imposed along the main flow path. This pressure drop is also the driving cause for the leakage flow through the brush seal that separates the high(front cavity) and low(back cavity) pressure zones.

2.1. Governing Equations

The 3-D Navier-Stokes equations(Schlichting(1978)) are applied here, while we are assuming rotational symmetry of the flow. To account for the pressure drop in the mainstream across the vane row, we introduce a local flow resistance in the form of the Darcy's Law. Thus, the permeability coefficient k_x is calculated based on apriori specified data regarding the pressure drop across the vane's blade row, Eq. 1a.

Main Flow path and Cavity Space. In view of the above, the governing equations for the fluid flow in the disk cavity and along the mainstream flow path can be formulated in dimensionless conservative form as

$$\frac{\partial u}{\partial t} + \frac{\partial (vu)}{\partial r} + \frac{\partial (uu)}{\partial x} = - \frac{\partial p}{\partial x} + \frac{1}{Re}\left(\frac{\partial^2 u}{\partial r^2} + \frac{1}{r}\frac{\partial u}{\partial r} + \frac{\partial^2 u}{\partial x^2}\right) - \frac{1}{k_x Re}\, u\, \delta_{xy} \tag{2}$$

$$\frac{\partial v}{\partial t} + \frac{\partial (vv)}{\partial r} + \frac{\partial (uv)}{\partial x} - \frac{(w)^2}{r} = - \frac{\partial p}{\partial r} + \frac{1}{Re}\left(\frac{\partial^2 v}{\partial r^2} + \frac{\partial}{\partial r}\left(\frac{v}{r}\right) + \frac{\partial^2 v}{\partial x^2}\right) \tag{3}$$

$$\frac{\partial w}{\partial t} + \frac{\partial (vw)}{\partial r} + \frac{wv}{r} + \frac{\partial (uw)}{\partial x} = \frac{1}{Re}\left(\frac{\partial^2 w}{\partial r^2} + \frac{\partial}{\partial r}\left(\frac{w}{r}\right) + \frac{\partial^2 w}{\partial x^2}\right) \tag{4}$$

For such systems, the pressure equation was determined by Ivanushkin et al., (1980) using the momentum equation integration technique first described by Welch et al., (1966) and then exemplified by Roache(1982) in its the application to a Cartesian coordinates geometry. Thus, one can write

$$\frac{\partial^2 p}{\partial x^2} + \frac{1}{r}\frac{\partial p}{\partial r} + \frac{\partial^2 p}{\partial r^2} = - \left(\frac{\partial^2 (u^2)}{\partial x^2} + \frac{\partial^2 (v^2)}{\partial r^2} + 2\frac{\partial^2 (uv)}{\partial x \partial r} + 2\frac{v^2}{r^2} \right) - \left(\frac{\partial D}{\partial t} + u\frac{\partial D}{\partial x} + v\frac{\partial D}{\partial r}\right) + \frac{1}{Re}\left(\frac{\partial^2 D}{\partial x^2} + \frac{1}{r}\frac{\partial D}{\partial r} + \frac{\partial^2 D}{\partial r^2}\right) + \frac{\partial}{\partial r}\left(\frac{w^2}{r}\right) + \frac{1}{k_x Re}\frac{\partial u}{\partial x}\,\delta_{xy} \tag{5}$$

where D is the dilation term

$$\frac{\partial v}{\partial r} + \frac{v}{r} + \frac{\partial u}{\partial x} = D \tag{6}$$

In Eqs. 2 and 5 $\delta_{xy} = 1$ for the vane's blade row flow area, while $\delta_{xy} = 0$ for the rest of the computational domain.

The Brush Region. For this portion of the flow additional modifications were introduced into the main system of governing equations (Eqs. 2-6). To provide an improved solution at the interface between the brush seal and the adjacent high and low pressure cavities we have introduced: a) the Brinkman Extension of Darcy's model for the porous area occupied by the brush seal bristles, and b) the conservative formulation of the convective and diffusion terms that also include porosity of the brush seal.

The resulting momentum equations for the brush region are:

$$\frac{1}{\epsilon}\frac{\partial u}{\partial t} + \frac{\partial (vu/\epsilon^2)}{\partial r} + \frac{\partial (uu/\epsilon^2)}{\partial x} = - \frac{\partial p}{\partial x} + \frac{1}{Re\,\epsilon}\left(\frac{\partial^2 u}{\partial r^2} + \frac{1}{r}\frac{\partial u}{\partial r} + \frac{\partial^2 u}{\partial x^2}\right) - \frac{u}{k_u Re} \tag{7}$$

$$\frac{1}{\epsilon}\frac{\partial v}{\partial t} + \frac{\partial (vv/\epsilon^2)}{\partial r} + \frac{\partial (uv/\epsilon^2)}{\partial x} - \frac{(w)^2}{r} = - \frac{\partial p}{\partial r} + \frac{1}{Re\,\epsilon}\left(\frac{\partial^2 v}{\partial r^2} + \frac{\partial}{\partial r}\left(\frac{v}{r}\right) + \frac{\partial^2 v}{\partial x^2}\right) - \frac{v}{k_v Re} \tag{8}$$

$$\frac{1}{\epsilon}\frac{\partial w}{\partial t} + \frac{\partial (vw/\epsilon^2)}{\partial r} + \frac{wv}{r} + \frac{\partial (uw/\epsilon^2)}{\partial x} = \frac{1}{Re\,\epsilon}\left(\frac{\partial^2 w}{\partial r^2} + \frac{\partial}{\partial r}\left(\frac{w}{r}\right) + \frac{\partial^2 w}{\partial x^2}\right) - \frac{w}{k_w Re} \tag{9}$$

In a view of the modifications of the momentum equations the pressure equation takes now the form

$$\frac{\partial^2 p}{\partial x^2} + \frac{1}{r}\frac{\partial p}{\partial r} + \frac{\partial^2 p}{\partial r^2} = - \left(\frac{\partial^2 (u^2/\epsilon^2)}{\partial x^2} + \frac{\partial^2 (v^2/\epsilon^2)}{\partial r^2} + 2\frac{\partial^2 (uv/\epsilon^2)}{\partial x \partial r} + \frac{2}{\epsilon}\frac{v^2}{r^2} \right) - \left(\frac{1}{\epsilon}\frac{\partial D}{\partial t} + u\frac{\partial D}{\partial x} + v\frac{\partial D}{\partial r}\right) + \frac{1}{Re\,\epsilon}\left(\frac{\partial^2 D}{\partial x^2} + \frac{1}{r}\frac{\partial D}{\partial r} + \frac{\partial^2 D}{\partial r^2}\right) + \frac{\partial}{\partial r}\left(\frac{w^2}{r}\right) + \frac{1}{k_u Re}\frac{\partial u}{\partial x} + \frac{1}{k_v Re}\frac{\partial v}{\partial r} \tag{10}$$

where D is a slightly modified dilation term

$$\frac{\partial (\epsilon v)}{\partial r} + \frac{\epsilon v}{r} + \frac{\partial (\epsilon u)}{\partial x} = D \tag{11}$$

where $k_{u,v,w}$ are the three nondimensional permeability coefficients (Darcy numbers) of the brush seal with respect to the different directions. On inspection of Eqs. 6 through 10 one notices that k, also called the Darcy number, plays quite a prominent role principally characterizing the sealing capability of the brush. Accuracy in its determination is important, and can be established via three different methods.

The Numerical Approach. This approach requires numerical modeling of the Navier-Stokes equations through the brush segment, Fig. 2, following the methodology described by Braun and Kudriavtsev (1992,1993a,b), obtaining values of the average pressure drops, and finally calculating permeability using Eq. 1a.

The Theoretical Approach. Brush permeability can be calculated using Ergun's(1952) formula

$$k = \frac{d^2 \epsilon^3}{A(1-\epsilon)^2} \tag{12}$$

where A=150. Kuwahara et al., (1994) performed numerical studies of a matrix of 10x10 inclined cylinders and squares. It was found that the calculated permeability is almost identical to the (linear term) variable k in Ergun's equations (Eqs.12, 13). The authors determined that A=153 when $\epsilon \in$ (0.08-0.84) for the square rods, and A=143 when $\epsilon \in$ (0.5-0.75), for the circular rods. It was found that two-dimensional and three-dimensional models lead to almost identical expressions for permeability(Kuwahara et. al (1994)). The format of the empirical Ergun's expression(1952) allows to account also for the variation of a brush packing density under real engine conditions, i.e. variable pressure difference across the seal.

$$-\frac{dP}{dx} = \frac{A(1-\epsilon)^2}{d^2\epsilon^3}\mu U_D + \frac{0.143\, U^2_D}{\epsilon^{3/2}\, k^{1/2}} \tag{13}$$

From Eq. 13 one can see that for constant bristle diameter(d), the Darcian leakage velocity U_D is a direct function of the average porosity and pressure differential. The change in the pressure differential is linked with the change in average porosity due to the deflection of the bristles under the pressure. Thus, we can account for the potential movement of the bristles through the change in porosity ϵ.

The Experimental Approach. Experimental leakage flow data can be used to obtain brush seal effective permeability using Eq. 1a. In this case dP/dX is an experimental pressure gradient that is function of the brush thickness. However, in this case we will obtain "effective" seal permeability, since a large component of the leakage flow rate comes through the clearance between the brush and rub-runner, while the backing and front plates impose an additional flow resistance. Materials presented in the paper of Carlile et al., (1993) provide enough information for estimation of a brush seal permeability coefficient k_u.

2.2. Boundary conditions.

In Fig. 1a one can find a sketch of the computational domain with specified boundary conditions. The main flow enters the computational domain with zero radial velocity v, zero circumferential velocity w(preswirl), and an axial velocity u=1. The normalizing reference velocity is U_o=100 m/s. The maximum rotational velocity at the disk tip is w=1 where again, the normalizing velocity is U_o=100 m/s. The rotational velocity along the radial disk walls is a linear function of the radial coordinate

$$w(r) = r/\, r_m \, * w_{top} \quad (\text{where } w_{top}=u_{top}=1) \tag{14}$$

The rotational velocity at the shaft surface(bottom of a cavity) is constant

$$w_{shaft} = r_{shaft}/\, r_m \, * w_{top} \tag{15}$$

where r_m is cavity (disk) tip radius and r_{shaft} is shaft radius. On the surface of the stationary vane u=v=w=0. At the main stream outflow, one can impose $\frac{\partial v}{\partial x}=\frac{\partial w}{\partial x}=0$, which accounts for developed flow conditions, and the axial velocity gradient is calculated through the mass balance of the continuity equation

$$\frac{\partial u}{\partial x} = -\left(\frac{\partial v}{\partial r} + \frac{v}{r}\right) \tag{16}$$

The pressure boundary conditions on the stationary walls are determined from the momentum equations, assuming that u=v=w=0. Thus

$$\frac{\partial p}{\partial x} = \frac{1}{Re}\left(\frac{\partial^2 u}{\partial r^2} + \frac{1}{r}\frac{\partial u}{\partial r} + \frac{\partial^2 u}{\partial x^2}\right) \tag{17}$$

$$\frac{\partial p}{\partial r} = \frac{(w)^2}{r} + \frac{1}{Re}\left(\frac{\partial^2 v}{\partial r^2} + \frac{\partial}{\partial r}\left(\frac{v}{r}\right) + \frac{\partial^2 v}{\partial x^2}\right) \tag{18}$$

Since at the interstage cavity inlet(Fig. 1a) u=1=const and v=0, one can write

$$\frac{\partial p}{\partial x} = -u\frac{\partial u}{\partial x} + \frac{1}{Re}\frac{\partial^2 u}{\partial x^2} \tag{19}$$

At the cavity exit(Fig. 1a)

$$\frac{\partial p}{\partial x} = -v\frac{\partial u}{\partial r} - u\frac{\partial u}{\partial x} + \frac{1}{Re}\left(\frac{\partial^2 u}{\partial r^2} + \frac{1}{r}\frac{\partial u}{\partial r} + \frac{\partial^2 u}{\partial x^2}\right) \tag{20}$$

Thus the pressure conditions are calculated along all the boundaries of the computational domain using Neumann type boundary conditions.

In the gas turbine the flow along the main flowpath is driven due to the pressure difference between the nozzle guide vane and the turbine exhaust. For the interstage cavity under consideration the most part of the pressure drop in the area where the vane blade row is located. In the 2D formulation it is not possible to account for this effect. We used a distributed flow resistance (in the Darcy law format) to account for this pressure drop along the main flow path.

2.3. Solution Parameters

The model using the governing equations presented above has been applied to a geometry that is characterized by the parameters tabulated in TABLE 1.
For this study we had chosen constant permeability k_u=6.0 x10^{-13} . One can obtain this value by using Eq. (12) with ϵ=0.216 and d=0.075 mm.

2.4. Computational Grid.

A nonuniform grid 207x145 (Fig. 1c) was superimposed over the computational domain of Fig. 1a. In order to provide enhanced flow resolution the grid had an increased density near the cavity walls and in the area adjacent to the brush seal. Numerical experiments indicated that this grid size constituted the minimum requirement for the accurate resolution of the complex vortex separation processes that are taking place within the interstage cavity. The overall grid contained 23 separate regions along the axial direction, and 14 such regions along the radial direction. Inside each one of these regions the grid steps are uniform, but different from region to region. Figure 1c presents the computational mesh used for all the flow simulations discussed in this paper. The sketch of the grid imposed over the domain of the brush seal is shown in Fig. 1b.

2.5. Details of the Solution Procedure

The solution of the system of governing equations introduced above, follows the use of the time dependent alternating direction implicit method (ADI) applied to the nonuniformly distributed collocated grid, Figs. 1b, and 1c. The procedure uses the full direct approximation of each term within the differential equation on every half time step, $\Delta\tau/2$(Braun and Kudriavtsev(1993, 1994). The spatial derivatives, with the exception of the convection terms and cross-derivatives, are approximated by a second-order central finite difference. For the convection terms the first-order conservative scheme proposed by Torrance(1968) is employed. The solution which employs a tridiagonal matrix e

TABLE 1
Physical Characteristics and Parameters used in the Numerical Computations

Brush seal Darcy number	Da=k_u=6 x10^{-7}
Rotational ratio	R=w_{max}/U_{in}=1.
Main flow Reynolds number	Re_m=1.2 x 10^5
Vane flow Darcy number	Da=k_x=10^{-4}
Computational domain dimensions:	
Normalizing length	L_0=1 mm,
Nondimensional Axial size	l_x=28.1
Nondimensional Radial size	l_r= 34.48
Nondimensional Shaft Radius	r_{shaft} =160.0
Nondimensional Tip Cavity Radius	r_m=183.48
Brush seal characteristics:	
Brush permeabilities	$\epsilon=k_u/k_v$=0.01
Permeability (k_x)	k_{Ergun}=6.0 x 10^{-13}
	k_{exp}= 5.0 x 10^{-13}
[k_{exp} calculated from Carlile, Hendricks & Yoder(1993) data].	
Bristle diameter	d = 0.075 mm
Brush seal porosity	ϵ=0.216
Brush seal clearance	l_{cl}=0.08 mm

elimination(TDMA) marches through the following steps:

- solve in the x direction for U velocity at the n+1/2 time step,
- solve in the y direction for the U velocity at the n+1 time step,
- solve in the x direction for V velocity at the n+1/2 time step,
- solve in the y direction for the V velocity at the n+1 time step,
- solve in the x direction for W velocity at the n+1/2 time step,
- solve in the y direction for the W velocity at the n+1 time step,
- solve the Poisson's pressure equation at the n+1 time step by means of the pseudo-transient method within the set of internal ADI iterations n_{it}=1,...n_f:
  - (i) in the x direction at the s+1/2 pseudo-time step, and
  - (ii) in the y direction at the s+1 pseudo-time step.
- proceed to the next time step.

Note that the pressure equation is solved until convergence is achieved in the internal iteration loop on every time step(global iteration). The set of Eqs. 2 through 6 which characterize the flow in the main stream and the cavity is automatically replaced by the set of Eqs. 7 through 11 when the TDMA sweeps are passing through the nodal points that belong to the brush seal. No special procedures are required to interface between the brush seal and interstage cavity. The conservative formulation of Eqs. 6 to 10 is sufficiently conditioned in combination with the variable grid increased density, to allow numerical stability throughout the entire domain.

3. RESULTS AND DISCUSSION

In Figs. 3a, and 3b one can find the global flow patterns that occur in the interstage cavities presented in Fig. 1. Figure 3a shows the flow when the side disk walls of the cavity are rotating, while Fig. 3b presents the version of the same flow when the velocity of the side walls is zero. These flows, whether they contain or not the disks rotational effects, are generally extremely complicated even for the simplified geometry used here. One can see four interacting vortices of different sizes in the front cavity, three major vortices in the seal cavity, several more vortices and a shear layer in the downstream cavity. The three vortices in the vane cavity are generated by the shear layer that fills the smaller downstream cavity. A small gap induced recirculation zone(GRZ) similar to the one presented by Ko et al., (1993) and Guo et al., (1994) is present in the area where the vane cavity is bound by the main flow stream. Generation of this zone provides the mechanism by which flow leaves the back cavity. A comparison between the flow patterns of Fig. 3a and Fig. 3b indicates a slight increase in the vortex structure complexity when rotation is not present; also the corner vortices that are located near the rotating walls are much stronger. Thus, it appears that for the geometry and flow parameters that were considered in this study, the rotational effects have limited influence on the global interstage cavity flow structure. To further support this conclusion we present in Fig. 3c the contour images of the flow field when the side walls are rotating. The dark area zones are indicative of regions that have not heen penetrated by the effects of the rotating side disks, and thus the w-component of the velocity is still close to zero. One can also see that since the mainstream w-velocity field was set equal to zero(boundary conditions), the main stream ingress into the interstage cavity areas prevents the development of strong rotation effects. Note that rotational components are strong only in the lower corners of the interstage cavity. It is also worth mentioning that in the area surrounding the brush seal, the flow rotational component is considerably diminished in value.

In Figs. 4a, and 4b one can see details that reveal the flow structure in the brush seal area for the cases with rotating(Fig. 4a), and respectively non-rotating side walls(Fig. 4b). One can again appreciate the complex flow formations that are taking place in the area where the brush seal is located. Because of the brush high resistance to flow passage, part of the secondary flow is reversing its direction towards the rotating wall. This effect becomes especially strong when the front cavity wall is rotating. It can be seen that the flow entering the area between the front plate and the shaft is skewed and generally non-uniform. A major part of this flow is heading towards the clearance, where the velocity magnitude is several times higher than elsewhere. Part of the flow enters the brush(porous medium), and starts a slow motion along the hrush walls. First downward and inside, and then upward, outside of the brush backing plate(BP). From Figs.4a, and 4b we can clearly see that the radial component of the brush flow is comparable in size to the axial component. Thus the assumption that the radial component is negligible and the brush flow can be represented by the flow pattern of an axial cross-section, clearly does not hold. If one studies further the area near the BP and the gap between the BP and the shaft, one finds very complex flow structures, probably real, that could never be visualized if a set of simplified calculations(uniform inflow and specified outflow boundary conditions), or bulk calculations were made. We refer in particular to the secondary vortex that is splitting behind the BP, with part of it entering the gap area, meeting the leakage flow and reversing its direction.

The powerful leakage flow stream, is instrumental in shaping the flow pattern that fills the seal cavity, Figs. 5 and 6. This flow stream remains attached to the shaft surface, whether the shaft rotates or not. Note that the cavities' lateral walls are attached to the shaft, and when the shaft rotates so do the side walls. Figures 5a, and 5b demonstrate different flow patterns that appear in the seal cavity as the process progresses in time. The flow is completely past the transient developmental stage(from rest to steady state). However, its shape keeps evolving in time, proving that while a steady state is not existent, a quasi steady-state, somewhat periodic behavior has set in. When the shaft is rotating, Fig. 5a, we can clearly observe three secondary vortices of continuous and periodic changing flow patterns, which exchange momentum by means of the appearance and disappearance of the small middle vortex. In the case of the stationary shaft, Fig. 5b, one can distinguish two main secondary vortices. The second one of the two exhibits an elongated backward moving finger that interposes between the first main vortex and the leakage flow stream emerging from under the brush. The rotation of the shaft seems to stimulate the development of the two main vortices,

and suppresses the minor vortices and their effects.

Extremely interesting is the flow formation that appears under high shaft rotation, and small flow leakage from the brush. Figure 5c presents just such a case. The decrease in leakage can follow from a strong reduction in seal clearance or decreased brush permeability. The disappearance of the strong axial flow along the shaft allows the formation of Taylor vortices, between the inner rotating shaft and outer stationary cylinder(vane). This form of fluid instability creates three almost equal length vortices that fill the entire cavity between the vane and the rotating shaft. In effect, the apparition of the Taylor formations indicate the domination of the rotational effects upon the axial flow shear layer that contains the leakage fluid. Again, it is proven that the integrated cavity/seal approach allows increased insight in the many complicated flow features that are influencing the global flow field.

Figure 6 delivers a very intuitive insight into the effect of the rotating shaft on the patterns and penetration of the rotational effect into the flow of the seal cavity. The periodic nature of the flow can be observed again, together with the fact that the zone of higher rotational component(white color) penetrates inside the cavity, increasing its size, Figs. 6.1, 6.2, and 6.3, only to start returning to its initial size and location, as the flow cycles (Figs. 6.4, 6.5, 6.6, and 6.7) .

Quantitative mapping of the pressure development in the front and back cavities as well as in the seal cavity, Figs. 7a, 7b, and 7c support our qualitative conclusion that flow in the interstage cavity is periodic in nature. Thus, Fig. 7a shows variations of the pressure drop across the hrush seal and in-between the front and back cavities. One can clearly assess the periodic variation of the pressure that is associated with a corresponding variation in the flow patterns. Figure 7b demonstrates the periodic behavior of the maximum velocity in the brush seal clearance area and at the seal cavity outflow boundary. In Fig. 7c the periodic nature of the rotational component in the front cavity is on display. Corroborated, all these data allows the important conclusion, that for high main flow Reynolds numbers(always the case in the gas turbine flow path) the fluid flow has a periodic oscillatory nature that require time-dependent terms in the governing equations. These terms are routinely omitted by some researchers (Ko et al., (1993), Iacovidies and Launder(1991), Guo et al., (1994)).

CONCLUSIONS

The present paper presents work-in-progress results and model developments that are directed towards the computational fluid dynamics simulation of the secondary flow system of the gas turbine engine. A computational algorithm and computer program (FLOCON) has been developed to model complex interstage gas turbine cavity flow with the brush seal inserted between adjacent cavities. A combination of two flow models, the first, for the brush seal(porous media assumption), and the second, for the interstage cavity(rotational axisymmetric flow) was successfully implemented into a single computational entity.

The pressure drop imposed along the vane row was used to create the driving force for the secondary flow system. The proposed integrated approach allows solutions for complex flow features that otherwise would not be accounted for. The results of the present study indicate that for some conditions rotational effects may be of minor effect for the brush seal flow and the global flow pattern. It was found that the flow in the hrush seal penetrates inside the porous brush body and has stronger near wall(backing and front plates) absolute velocities. Also, the axial velocity component is comparable with the radial velocity component due to lower flow resistance along the bristles. This fact brings up the conclusion that brush seal modeling when the brush is only represented by its axial (horizontal) cross-section is not self supporting.

In general, it was found that flow in the cavity has periodic nature, for both pressure, velocity and vortex formations.

REFERENCES

Athavale, M.M., Przekwas, A.J., Hendricks, R.C., 1993, "Driven Cavity Simulation of Turbomachinery Blade Flows with Vortex Control", AIAA-93-0390, 31st Aerospace Sciences Meeting & Exhibit, Jan 11-14, 1993, Reno, NV

Braun, M.J., Kudriavtsev, V.V., 1993a, "A Numerical Simulation of a Brush Seal Section and Some Experimental Results", Int. Gas Turbine and AeroEngine Congress, Cincinnati, 1993, ASME Paper 93-GT-398, 1-12, (also Transactions of the ASME, Journal of Turbomachinery, Vol. 117, No.1, Jan. 1995, pp. 190-202)

Braun, M.J., Kudriavtsev, V.V., 1993b, "Numerical Visualization of Flow Structures in Dense Banks of Cylinders Located in a Channel", Third Int. Symposium on Experimental and Numerical Flow Visualization, 1993 ASME Winter Annual Meeting, New Orleans, Louisiana, Nov. 28 - Dec. 3, 1993/Eds. B. Khalighi, M.J. Braun, C.F. Freitas, D.H. Fruman, pp. 1-8, (accepted for the puhlication - ASME Journal of Fluids Engineering, March-1995)

Braun M.J., Kudriavtsev, V.V., 1992, "Experimental and Analytical Investigation of Brush Seals", Seals Flow Code Development-92, NASA CP-10124, Proceedings of a workshop held at NASA Lewis Research Center, August, 5-6, 1992, pp. 181-195.

Burmeister, L.C., 1993, "Convective Heat Transfer, John

Wiley & Sons, pp.44-51.

Carlile, J.A., Hendricks, R.C., Yoder, D.A., 1993, "Brush Seal Leakage Performance with Gaseous Working Fluids at Static and Low Rotor Speed Conditions", 1993, Journal of Engineering for Gas Turbines and Power, Vol. 115, pp. 397-403

Chew, J.W., 1985, "Computation of Convective Laminar Flow in Rotating Cavities", J. Fluid Mech., Vol.153, p.339

Chupp, R.E., Dowler, C.A., "Performance Characteristics of Brush Seals for Limited-Life Engines", 1993, Journal of Engineering for Gas Turbines and Power, Apr. 1993, Vol. 115, pp. 390-396

Chupp, R.E., Holle, G.F., Dowler, C.A., 1991, "Simple Leakage Flow Model for Brush Seals", AIAA Paper No. 91-1913

Chupp, R.E., Holle, G.F., 1994, "Generalizing Circular Brush Seal Leakage Through a Randomly Distributed Bristle Bed", ASME Paper 94-GT-71, International Gas Turbine and AeroEngine Congress & Exposition, The Hague, Netherlands, June 13-16, 1994

Ergun, S., 1952, "Fluid Flow Through Packed Columns", Chem. Eng. Prog., Vol.48, No.2, pp. 89-94

Farthing, P.R., Long, C.A., Owen, J.M., Pincombe J.R., 1992, "Rotating Cavity with Axial Throughflow of Cooling Air: Flow Structure", ASME Journal of Turbomachinery, Vol. 114, pp. 237-246

Guo, Z., Rhode, D.L., Davis, F.M., 1994, "Computed Eccentricity Effects on Turbine Rim Seals at Engine Conditions with a Mainstream", ASME-94-GT-31, Int. Gas Turbine and Aeroengine Congress & Exposition, The Hague, Netherlands, June 13-16, 1994

Hendricks, R.C., Schlumberger, J., Braun, M.,J., Choy, F.C., Mullen, R.L., 1991, "A Bulk Flow Model of a Brush Seal System", ASME Paper No. 91 GT-325, 36th ASME International Gas Turbine and Aeroengine Congress & Exposition, Orlando, FL, June 3-6

Iacovides, H., Launder, B.E., 1991, "Parametric and Numerical Study of Fully Developed Flow and Heat Transfer in Rotating Rectangular Ducts", Journal of Turbomachinery, Jul. 1991, Vol. 113, pp. 331-338

Ivanushkin, S.G., Kim, L.V., Kondrashov, V.I., Tomilov, V.E., 1980, "Internal Transient Problems of Convective Heat Transfer", Tomsk University Publishers, Tomsk, pp. 1-150 (in Russian)

Ko, S.H., Rhode, D.L., Guo, Z., 1993, "Computed Effects of Rim Seal Clearance and Cavity Width on Thermal Distributions", ASME Paper 93-GT-419

Kudriavtsev, V.V., 1993, "Numerical Analysis of the Transient Fluid Flows in the Brush Seal Elements of the Aerospace Turbomachinery", Ph.D. Dissertation, Moscow Aviation Institute (in Russian)

Kudriavtsev, V.V., Braun, M.J., 1994, "Advances in Brush Seal Numerical Modeling", SAE Aerospace Atlantic '94 Conference and Exposition, SAE-TP-941208, /Advanced Dynamic Seals, Dayton, Ohio, pp.1-13 (Also AIAA Journal of Propulsion and Power, to be published in 1996).

Kuwahara, F., Nakayama, A., Koyama, H., 1994, "Numerical Modelling of Heat and Fluid Flow in a Porous Medium", Heat Transfer, 1994, Vol.5., Proceedings of the Tenth International Heat Transfer Conference, Brighton, UK, Paper-11-PP-18, pp. 309-314,

Ong, C.L., Owen, J.M., 1991, "Prediction of Heat Transfer in a Rotating Cavity with a Radial Outflow", ASME Journal of Turbomachinery, Vol. 133, pp.115-122

Owen, J.M., Onur, H.S., 1983, "Convective Heat Transfer in a Rotating Cavity", ASME Journal of Engineering for Power, v. 105, pp. 265-271

Przekwas, A.J., Athavale, M.M., Hendricks, R.C., 1994, "Progress in Advanced Modeling of Turbine Engine Seal Flows", AIAA-94-2803, 30th Joint Propulsion Conference

Roache, P.L., 1982, Computational Fluid Mechanics, Hermosa Publishers.

Schlichting, H., 1978, Boundary-layer Theory, N.Y., McGraw-Hill

Torrance, K.E., 1968, "Comparison of Finite-Difference Computations of Natural Convection", Journal Research NBS: Mathematical Sciences, N72B, 281.

Vaughan, C.M., Turner, A.B., 1987, "Numerical Prediction of Axisymmetric Flow in a Rotor-Stator System with an External Mainstream Flow", Proceedings 5th Int. Conf. on Numerical Methods in Laminar and Turbulent Flows, Swansea, UK.

Virr, G.P., Chew, J.W., Coupland, J., 1993, "Application of Computational Fluid Dynamics to Turbine Disk Cavities", ASME Paper No. 93-GT-89.

Welch, E.J., Harlow, F.H., Shannon, J.P., Daly, B.J., 1966, "The MAC Method: A Computing Technique for Solving Viscous, Incompressible, Transient Fluid Flow Problems Involving Free Surfaces", Technical Report, Los Alamos Scientific Laboratory, LA-3425,UC-32, TID-4500

ACKNOWLEDGEMENT

The authors want to express their gratefulness to Drs. Robert Bill, Robert Hendricks, and Mr. George Bobula from NASA Lewis Research Center, Cleveland, Ohio, for their continued support and encouragement. The work has been performed under the auspices of NASA Grant NAG 3-969, NASA Lewis Research Center.

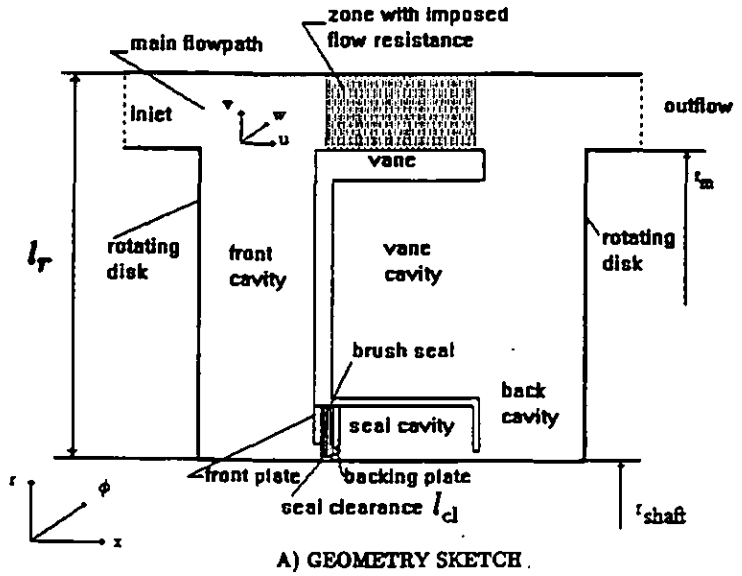

A) GEOMETRY SKETCH

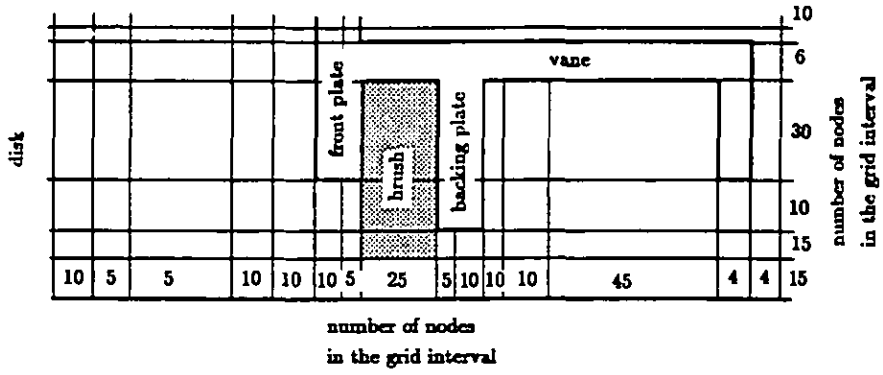

B) GRID INTERVALS AROUND THE BRUSH SEAL

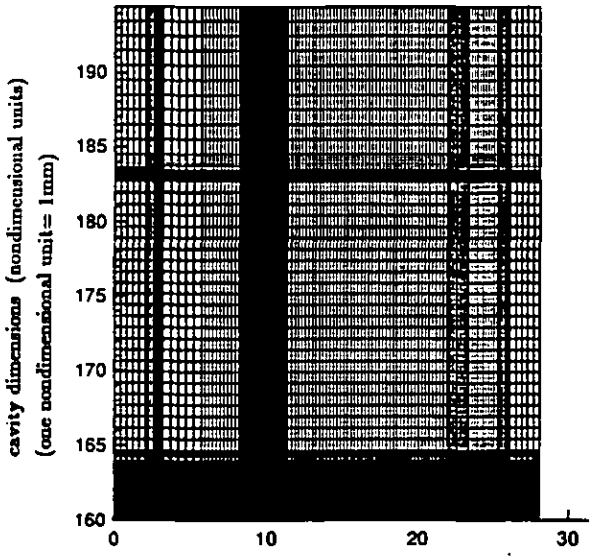

C) COMPUTATIONAL GRID (209 x144)

FIGURE 1(A,B,C). SIMULATED INTERSTAGE CAVITY

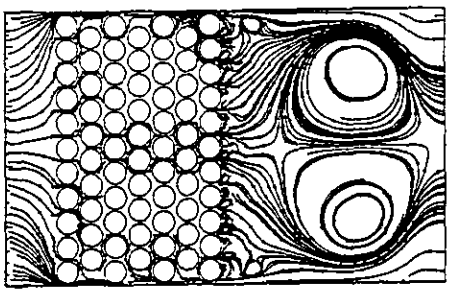

FIGURE 2. FLOW THROUGH THE SIMULATED BRUSH SEGMENT LOCATED IN THE CHANNEL

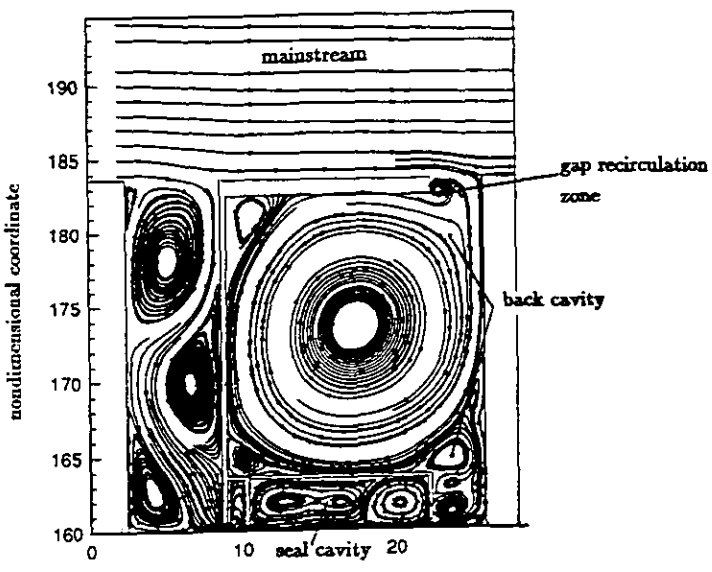

A) ROTATING CAVITY

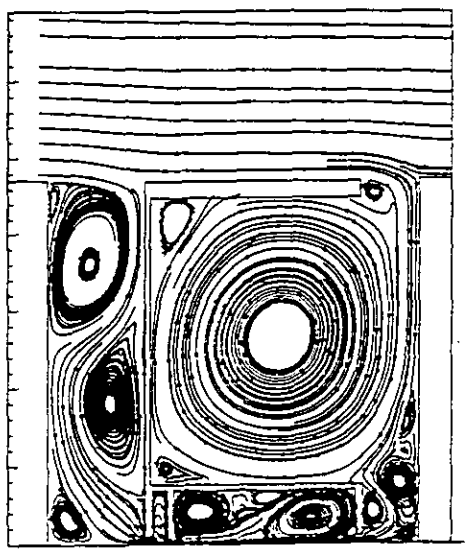

B)NONROTATING CAVITY

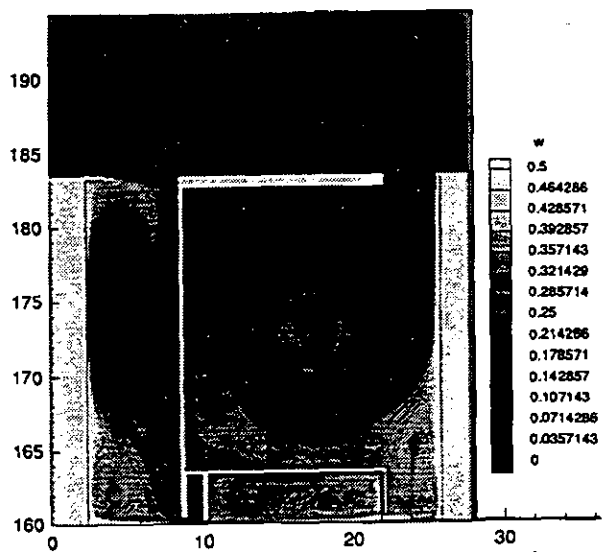

C) ROTATIONAL VELOCITY DISTRIBUTION

FIGURE 3 FLOW PATTERNS IN THE INTERSTAGE SEAL CAVITY

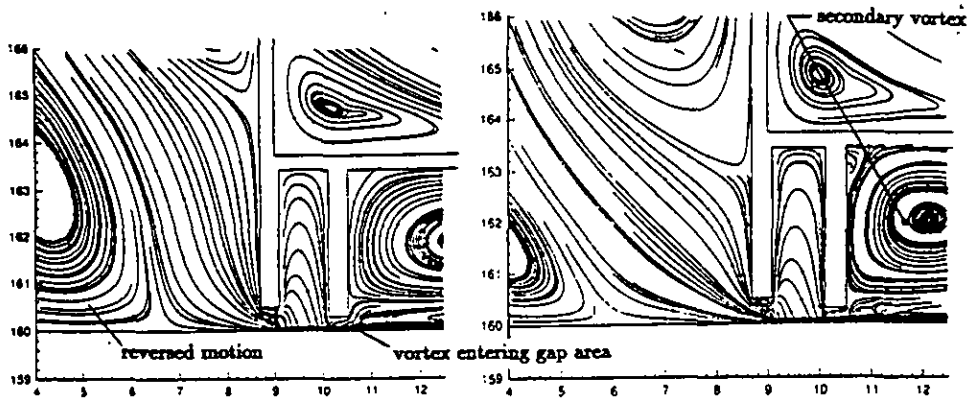

A) ROTATING CAVITY B)NONROTATING CAVITY

FIGURE 4(A,B) FLOWFIELD IN THE AREA SURROUNDING THE BRUSH SEAL

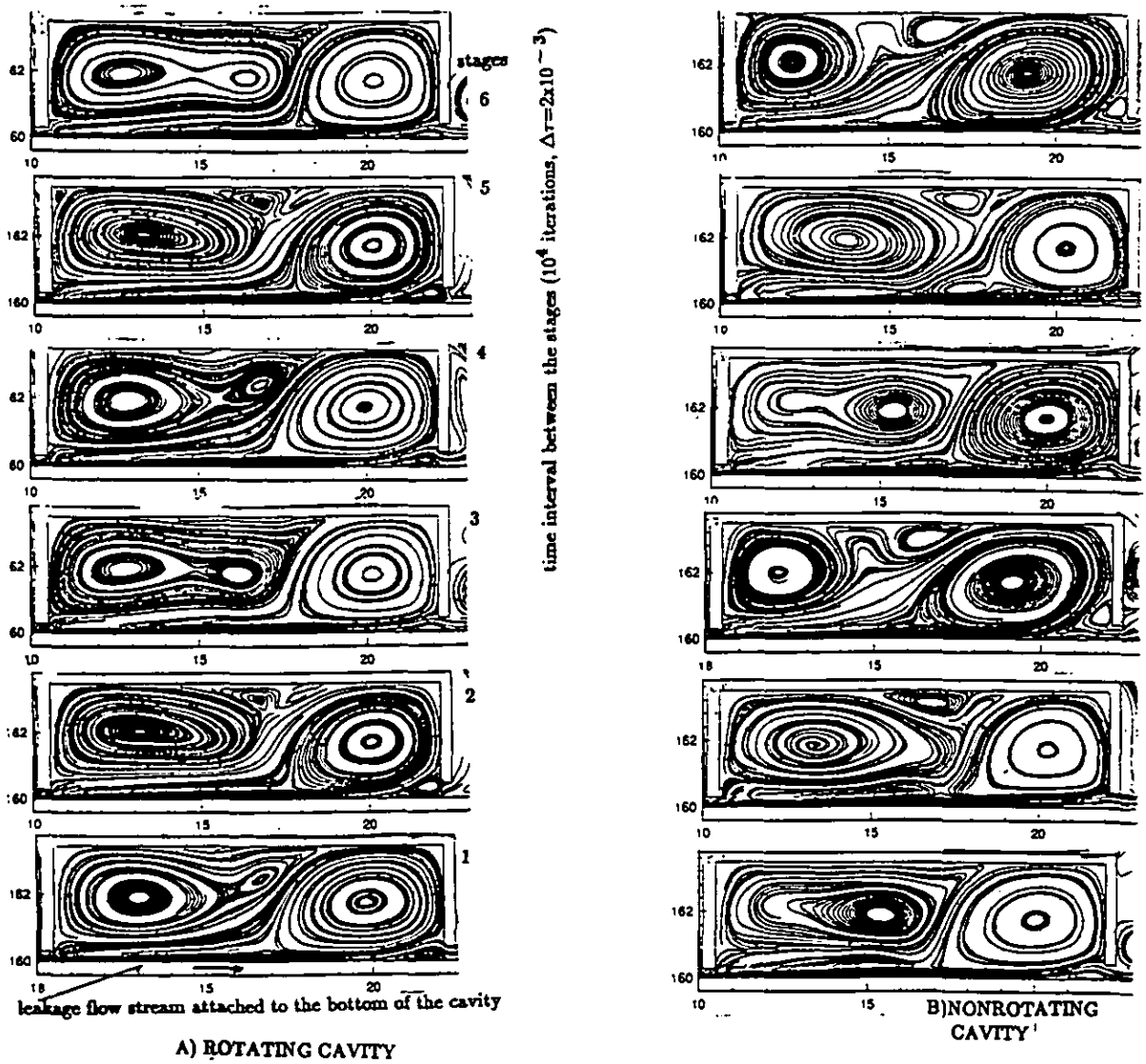

FIGURE 5(A,B,C). FLOW PATTERNS IN THE SEAL CAVITY

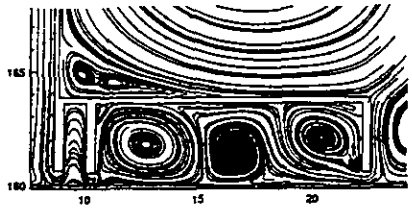

C) TAYLOR VORTICIES
(throughflow through the seal
is small)

FIGURE 5(A,B,C). FLOW PATTERNS IN THE SEAL CAVITY

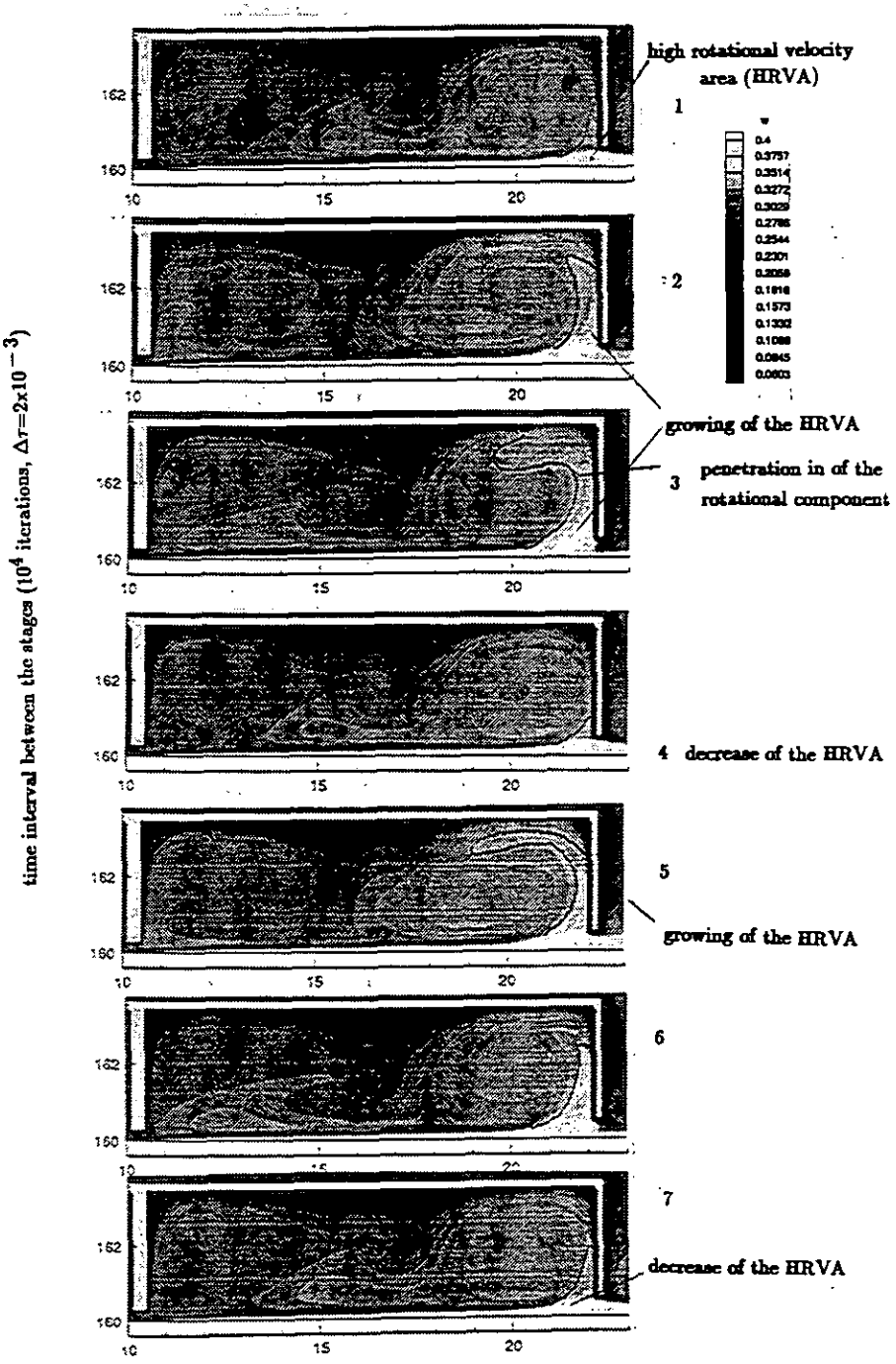

FIGURE 6. EVOLUTION OF THE ROTATIONAL FLOWFIELD IN THE SEAL

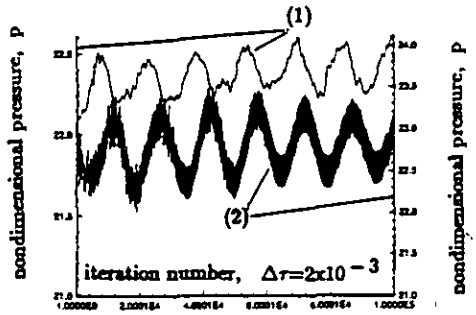

$P(\text{dimensional})=p \times \rho u^2_0$

A)PRESSURE DROPS ACROSS THE BRUSH SEAL (1) and BETWEEN THE FRONT AND BACK CAVITIES(2)

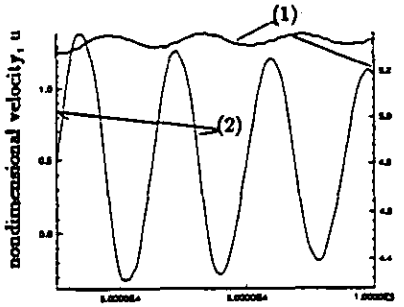

B)AXIAL VELOCITY COMPONENT U
(1) BRUSH SEAL CLEARANCE
(2) SEAL CAVITY OUTFLOW

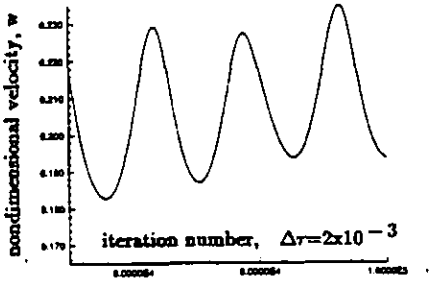

C) ROTATIONAL COMPONENT W (center of the front cavity)

FIGURE 7(A,B,C) PERIODIC FEATURES OF THE FLUID FLOW